Robotica (2009) volume 27, pp. 825–840. © Cambridge University Press 2008
doi:10.1017/S0263574708005183

Trajectory optimization of flexible link manipulators in point-to-point motion

M. H. Korayem*, A. Nikoobin and V. Azimirad

Robotic Research Laboratory, College of Mechanical Engineering, Iran University of Science and Technology, Tehran, Iran

(Received in Final Form: October 2, 2008. First published online: November 4, 2008)

SUMMARY

The aim of this paper is to determine the optimal trajectory and maximum payload of flexible link manipulators in point-to-point motion. The method starts with deriving the dynamic equations of flexible manipulators using combined Euler–Lagrange formulation and assumed modes method. Then the trajectory planning problem is defined as a general form of optimal control problem. The computational methods to solve this problem are classified as indirect and direct techniques. This work is based on the indirect solution of open-loop optimal control problem. Because of the offline nature of the method, many difficulties like system nonlinearities and all types of constraints can be catered for and implemented easily. By using the Pontryagin's minimum principle, the obtained optimality conditions lead to a standard form of a two-point boundary value problem solved by the available command in MATLAB®. In order to determine the optimal trajectory a computational algorithm is presented for a known payload and the other one is then developed to find the maximum payload trajectory. The optimal trajectory and corresponding input control obtained from this method can be used as a reference signal and feedforward command in control structure of flexible manipulators. In order to clarify the method, derivation of the equations for a planar two-link manipulator is presented in detail. A number of simulation tests are performed and optimal paths with minimum effort, minimum effort-speed, maximum payload, and minimum vibration are obtained. The obtained results illustrate the power and efficiency of the method to solve the different path planning problems and overcome the high nonlinearity nature of the problems.

KEYWORDS: Manipulator; Flexible link; Maximum payload; Optimal trajectory; Optimal control; Indirect solution; Boundary value problem.

1. Introduction

The manipulators are typically used to repeat a prescribed task a large number of times, so even small improvements in their performance may result in large monetary saving. This improvement can be achieved by obtaining the optimal path of the robot performing the specific task. Since many different ways are possible to perform the same task, this freedom of choice can be exploited judiciously to optimize a given performance criterion. During the past decades, a great deal of attention has been given to the problem of motion planning and control. Because of the complexity of the problem, researchers divide the robot control structure into two levels:[1,2] the upper level, called the path or trajectory planning, and the lower level, called the path tracking or path control. Motion planning involves generating the path and its time law, providing the controller's reference signal. Motion tracking, on the other hand, is concerned with improving the tracking of the reference signal.

Most techniques found in the scientific literature on the trajectory planning problem are based on the optimization of some parameter or some objective function. The most significant optimality criteria are minimum execution time; minimum energy or actuator effort; and minimum jerk. Besides the aforementioned approaches, some hybrid optimality criteria have also been proposed. Load carrying capacity is another objective function considered in order to achieve optimal usage of robot manipulator. The maximum allowable dynamic load (MADL) of a manipulator is defined as the maximum value of load which a robot manipulator is able to carry on a desired trajectory.[3] On the other hand, in point-to-point motions (e.g., pick-and-place operations); the end effector is free to move between two extremal positions. In this case, the planner tries to define the maximum value of payload, optimal trajectory, and the corresponding controls.[4] With the aim of increasing the MADL, the path planning problem has been solved for rigid manipulators[3–6] and flexible joint ones[7,8] by many researchers. Dynamic load carrying capacity of flexible link manipulators has also been studied in refs. [9–11]. In refs. [9, 10] a formulation based on Iterative Linear Programming (ILP) is presented to determine the MADL of flexible manipulators. Indeed, because of very lengthy, highly nonlinear, and coupled set of dynamic equations, the ILP method is not efficient to solve such problem, so in these papers flexibility is neglected in simulations.

Lately, research on flexible manipulators has received increased attention due to their several advantages over the rigid ones.[12] The main advantages of a flexible manipulator are their capability to assure faster motions and a higher ratio of payload to arm weight. However, due to the flexible nature of the system, their dynamic equations are highly nonlinear and complex. Therefore, the path planning of such systems is a much more complicated task than for the rigid manipulators or mobile robots. However, the problem

* Corresponding author. E-mail: hkorayem@iust.ac.ir

of motion planning becomes quite complex and requires specific schemes for its treatment. Two main families for solving this problem can be distinguished: direct and indirect methods.[2,13]

Direct methods are based on a discretisation of dynamic variables (states, controls) leading to a parameter optimization problem. Then, nonlinear optimization, evolutionary or classical stochastic techniques are applied to obtain optimal values of the parameters. In refs. [14–16], the motion profiles of the joints are defined as a Spline or polynomial functions. Then, the functions parameters are obtained in order to reduce the residual vibration of flexible manipulators at the end of the motion. Wang *et al.* have solved the optimal control problem with direct method using the B-Spline functions in order to determine the maximum payload of a rigid manipulator.[6] In ref. [17] path planning of a flexible manipulator is formulated as a discrete-time open-loop optimal control problem, the solution of which is done via discrete dynamic programming. Another direct technique which is used for flexible manipulators is ILP. Just as mentioned above, applying this method to flexible manipulators is a hard task. In the ILP method, the linearizing procedure and its convergence to the proper answer is a challenging issue, especially when nonlinear terms are large and fluctuating, e.g., in problems with consideration of flexibility in joints or links. Also, the dynamic programming is not efficient for optimal control problems with high-dimensional state-space because of the curse of dimensionality and menace of the expanding grid.[18] Consequently, direct methods are exhaustively time consuming and quite inefficient due to the large number of parameters involved,[19] especially when flexibility is added to the system.

On the other hand, indirect method is based on Pontryagin Maximum Principle (PMP)[20] which was first used to define the optimal control. It was first used to solve minimum time motion problems along specified paths. Then, it was extended to handle free motions as well.[21,22] The PMP is used also to treat directly the optimal dynamic motion planning problem. The optimality conditions for transfer modalities are expressed as a set of differential equations in the form of the boundary value problems. Indirect method is widely used as a powerful and efficient tool in analyzing the nonlinear system and path planning of different types of systems.[21–27] This technique is especially suitable in the cases where the system has a large number of degree of freedom or optimization of the various objectives is targeted. Recently, this method has been successfully employed in the path planning of flexible joint manipulators in ref. [8], for the actuated kinematic chains in ref. [25], for a large multibody system in ref. [26], and for low-thrust trajectory optimization in ref. [27]. The main challenge of this method is in solving the obtained two-point boundary value problem (TPBVP), for which nowadays powerful and efficient commands are available to solve it in different software such as MATLAB, C++, and FORTRAN. A number of methods exist for solving these problems including shooting, collocation, and finite difference methods. In this study, BVP4C command in MATLAB® which is based on the collocation method is used to solve the obtained problem. The details of the numerical technique used in MATLAB to solve the TPBVP are given in ref. [28].

In this paper indirect solution of the optimal control problem is exploited for path planning of flexible link manipulators. Using this method for determining the maximum payload optimal path of flexible link manipulators, which has not been done yet, will be practicable. In comparison with other methods, the open-loop optimal control method does not require linearizing the equations (in ILP method), differentiating with respect to joint parameters (in Spline method), and using of a fixed-order polynomial as the solution form. The dynamic equation is derived using the generalized Euler–Lagrange formulation and assumed modes method. Hamiltonian function for a proper objective function is formed, then using the PMP optimality necessary conditions are obtained. The obtained equations establish a TPBVP solved by numerical techniques. The general formulation to find the optimal path and the maximum payload at point-to-point motion is derived. After that the developed algorithm to obtain the optimal path for a given payload is discussed. Another algorithm for calculating the MADL and the corresponding optimal path is presented later. In order to validate the method, simulation test is carried out for a two-link flexible manipulator and the obtained results are compared with those reported in ref. [17]. The other simulations are performed to illustrate the efficiency of the proposed method to solve the different path planning problems.

2. Modeling of a Manipulator With Multiple Flexible Links

The generalized Euler–Lagrange formulation and assumed modes method is used to derive the dynamic equation of flexible manipulators. All the flexible links are assumed to be Euler–Bernoulli beams, where the shear-force-shortening effect and rotary inertia are neglected.[12,29] For a general n-link flexible robot, the vibration $v_i(x_i, t)$ of each link which describes the deflection of the ith link with respect to its undeflected configuration can be represented by a series form as

$$v_i(x_i, t) = \sum_{j=1}^{n_i} \phi_{ij}(x_i) q_{ij}(t), \quad i = 1, \ldots, n \tag{1}$$

where $v_i(x_i, t)$ is the bending deflection of the ith link at a spatial point $x_i (0 \le x_i \le L_i)$ and L_i is the length of the ith link. n_i is the number of modes used to describe the deflection of link i; $\phi_{ij}(x_i)$ and $q_{ij}(t)$ are the jth mode shape function and jth modal displacement for the ith link, respectively. Position and velocity of each point on link i can be obtained with respect to inertial coordinate frame using the transformation matrices between the rigid and flexible coordinate systems. After that, by considering the generalized coordinates of the manipulator which consists of two parts, the generalized coordinates of the rigid body motion of links $q_r = (q_1, q_2, \ldots, q_n)^T$ and generalized coordinates defining the deflection of the manipulator $q_f = (q_{11}, q_{12}, \ldots, q_{1n_1}, q_{21}, \ldots, q_{2n_2}, \ldots, q_{n1}, \ldots, q_{nn_n})^T$,

https://doi.org/10.1017/S0263574708005183 Published online by Cambridge University Press

the dynamic equation of flexible link manipulator is developed by using the Lagrangian assumed modes method[29] as follows:

$$\begin{bmatrix} m_{rr} & m_{rf} \\ m_{fr} & m_{ff} \end{bmatrix} \begin{bmatrix} \ddot{q}_r \\ \ddot{q}_f \end{bmatrix} + \begin{bmatrix} H_r(q_r, q_f, \dot{q}_r, \dot{q}_f) \\ H_f(q_r, q_f, \dot{q}_r, \dot{q}_f) \end{bmatrix} + \begin{bmatrix} G_r(q_r, q_f) \\ G_f(q_r, q_f) \end{bmatrix} = \begin{bmatrix} \tau \\ 0 \end{bmatrix}. \quad (2)$$

By defining the generalized forces as $U = \{U_i\} = \{\tau_1, \tau_2, \ldots, \tau_n, 0, \ldots, 0\}^T$ and, the generalized coordinate system as $Q = \{Q_i\} = \{q_1, q_2, \ldots, q_n, q_{11}, q_{12}, \ldots, q_{1n_1}, \ldots, q_{n1}, q_{n2}, \ldots, q_{nn_n}\}^T$, where $i = 1, \ldots, n_t = n + n_1 + n_2 + \ldots + n_n$, Eq. (2) can be written in compact form as

$$M\ddot{Q} + H(Q, \dot{Q}) + G(Q) = U, \quad (3)$$

where M is the mass matrix, H is the vector of Coriolis and centrifugal forces, and G describes the gravity effects. By defining the following vectors as

$$X_1 = \{x_{2i-1}\} = Q,\ X_2 = \{x_{2i}\} = \dot{Q},\ F_1 = \{f_{2i-1}\},$$
$$F_2 = \{f_{2i}\}; i = 1, \ldots, n_t \quad (4)$$
$$X = \{x_i\},\ F = \{f_i\};\ i = 1, \ldots, 2n_t,$$

Eq. (3) can be expressed in terms of the following state equation

$$\dot{X}_1 = F_1 = X_2; \quad \dot{X}_2 = F_2 = D(X_1)U + N(X_1, X_2), \quad (5)$$

where $D = M^{-1}$ and $N = -M^{-1}(H(X_1, X_2) + G(X_1))$. Then optimal control problem is to determine the generalized coordinate $X(t)$, and the joint torque $U(t)$ which optimize a well-defined performance measure when the model is given in Eq. (5). The mathematical formulation of the problem is given in the next section.

3. Formulation of the Optimal Control Problem

3.1. Statement of optimal control problem

Let Ω be the set of the admissible control torques. The optimization problem in the Bolza-form is to find the input $U^*(t) \in \Omega$ so that the manipulator in Eq. (5) minimizes a below objective function

$$J_0(U) = \frac{1}{2}\|e_p(t_f)\|^2_{W_p} + \frac{1}{2}\|e_v(t_f)\|^2_{W_v} + \int_{t_0}^{t_f} L(X, U)\, dt, \quad (6)$$

$$e_p(t_f) = X_1(t_f) - X_{1f},\ e_v(t_f) = X_2(t_f) - X_{2f};$$
$$L = 0.5\left(\|X_1\|^2_{W_1} + \|X_2\|^2_{W_2} + \|U\|^2_R\right). \quad (7)$$

In these equations, t_0 and t_f are known as the initial and final times, $\|X\|^2_K = X^T K X$ is the generalized squared norm, W_p and W_e are the symmetric, positive semi-definite $n_t \times n_t$ weighting matrices, W_1, W_2, and R are the symmetric, positive definite $n \times n$ matrices. X_{1f} and X_{2f} are desired values of generalized coordinate and their rates at the final time t_f. The designer can decide on the relative importance among the position, velocity, motion errors, and control effort by the numerical choice of W_1, W_2, W_p, W_v, and R which can also be used to convert the dimensions of the terms to consistent units. So, if $\bar{U}$ be a set of admissible control torque over the time interval $t \in [t_0 t_f]$, the optimal control problem is to obtain the $U^*(t) \in \bar{U}$, in order to minimize the objective criterion given by Eqs. (6) and (7), subject to the motion Eq. (5), while steering the states from initial boundary conditions to the final situations.

3.2. Necessary condition for optimality

Indirect method has been applied here to solve the optimal control problem. In this method by introducing the costate vector $\psi \in R^{2n_t}$, the Hamiltonian function of the system can be defined as follows:

$$H(X, U, \psi, m_p, t) = L(X, U, m_p) + \psi^T(t)F(X, U, m_p). \quad (8)$$

For the optimal trajectory $X^*(t)$ and $U^*(t)$, the PMP states that there exists a nonzero costate vector $\psi^*(t)$which the following condition along the optimal solution must satisfy[20]

$$\dot{X}^*(t) = \frac{\partial H}{\partial \psi}, \quad \dot{\psi}^*(t) = -\frac{\partial H}{\partial X}, \quad 0 = \frac{\partial H}{\partial U} \quad (9)$$

$$H(X^*, \psi^*, U^*, t) \le H(X^*, \psi^*, \bar{U}, t) \quad \text{for all}$$
$$t \in [t_0 \quad t_f] \quad \text{and} \quad U \in \bar{U}, \quad (10)$$

where the symbol (*) refers to the extremals of $X(t)$, $U(t)$, and $\psi(t)$; and $\bar{U}$ denotes the admissible control value. By defining the costate vector as $\psi_1 = \{\varphi_{2i-1}\}$, $\psi_2 = \{\varphi_{2i}\}$, $i = 1, \ldots, n_t$ and substituting Eq. (5) into Eq. (8); Eq. (9) can be rewritten as follows:

$$\begin{bmatrix} \dot{X}_1 \\ \dot{X}_2 \end{bmatrix} = \begin{bmatrix} X_2 \\ N(X_1, X_2) \end{bmatrix} + \begin{bmatrix} 0 \\ D(X_1) \end{bmatrix} U \quad (11)$$

$$\begin{bmatrix} \dot{\psi}_1 \\ \dot{\psi}_2 \end{bmatrix} = -\begin{bmatrix} \frac{\partial L}{\partial X_1} + \frac{\partial}{\partial X_1}[D(X_1)U + N(X_1, X_2)]^T \psi_2 \\ \frac{\partial L}{\partial X_2} + \psi_1 + \frac{\partial}{\partial X_2}[N(X_1, X_2)]^T \psi_2 \end{bmatrix} \quad (12)$$

$$\frac{\partial L}{\partial U} + D^T(X_1)\psi_2 = 0. \quad (13)$$

Equations (11) and (12) represent necessary conditions for a local minimum of the objective function. Their solution provides a candidate for the optimal solution. Since the control values are limited with upper and lower bounds, using (13) and (10), the controls can be expressed as follows:

$$U = \begin{cases} U^+ & -R^{-1}D^T\psi_2 > U^+ \\ -R^{-1}D^T\psi_2 & U^- < -R^{-1}D^T\psi_2 < U^+ \\ U^- & -R^{-1}D^T\psi_2 < U^- \end{cases}. \quad (14)$$

https://doi.org/10.1017/S0263574708005183 Published online by Cambridge University Press

The torque speed characteristic of D.C. motors may be represented by the following linear equation:[4]

$$U^+ = K_1 - K_2\dot{\theta};\ U^- = -K_1 - K_2\dot{\theta}, \qquad (15)$$

where $K_1 = [\tau_{s1}, \tau_{s2}, \ldots, \tau_{sn}]^T$, $K_2 = \mathrm{dig}[\tau_{s1}/\omega_{m1}, \ldots, \tau_{sn}/\omega_{mn}]$, $\dot{\theta} = [\dot{\theta}_1, \dot{\theta}_2, \ldots, \dot{\theta}_n]^T$, τ_s is the stall torque and ω_m is the maximum no-load speed of the motor. The final and initial states and the traveling time are fixed, therefore the boundary condition can be expressed as follows:

$$X_1(0) = X_{10},\ X_2(0) = X_{20};\ X_1(t_f) = X_{1f},\ X_2(t_f) = X_{2f}. \qquad (16)$$

Substituting for U from Eqs. (14) and (15) in Eqs. (11) and (12), a set of $2n_t$ ordinary differential equations is formed. While Eq. (16) expresses $2n_t$ boundary value conditions which n_t of them are defined at $t = t_0$, and n_t other one at $t = t_f$. The algorithm iterates on the initial values of the costate $\psi(0)$, until the given boundary conditions in Eq. (16) are satisfied with the desired accuracy ε. To put it another way, the following relation must be fulfilled in TPBVP solving:

$$\frac{1}{2}\|X_1(t_f) - X_{1f}\|^2_{W_p} + \frac{1}{2}\|X_2(t_f) - X_{2f}\|^2_{W_v} \le \varepsilon, \qquad (17)$$

where X_f is desired boundary condition at $t = t_f$ and $X(t_f)$ is the obtained values of states at $t = t_f$ as per the obtained initial values of costates ($\psi(0)$) in TPBVP solution.

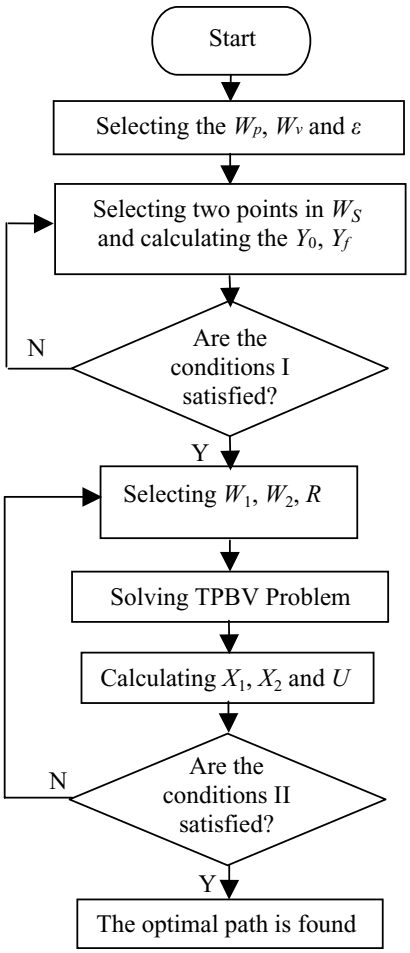

Fig. 1. Optimal path algorithm.

4. Determining the Optimal Path

4.1. Optimal path for a given payload

In more practical cases, the payload mass which is carried from the starting point to the end point is known. If the given task iterates in installments, by finding the optimal path between this two points, a large economic saving can be obtained. The optimal control approach provides a powerful tool for designers to create various optimal paths via defining the proper performance measure. For the cases where only one parameter (e.g., time, energy, or effort) is wanted to minimize, choosing the performance measure is straightforward. But when objective function consists of different terms (e.g., time and energy or torque and speed), choosing the weighting factors are not so easy. In this case, after initially adjusting the weighting factors in such a manner that the dimensions of different terms convert to consistent units, the problem is solved and the designer analyzes the results. So that for each nonsatisfied objective, the corresponding weighting factor must be increased or decreased with the purpose of reaching the desirable goal. The values of penalty matrices have a direct effect on the corresponding terms. For example, if decreasing the angular velocity in the second motor is wanted, the value of w_{22} in W_2 must be increased, and if the torque deduction of the first motor is required, the value of r_{11} in R must be greater than before.

An algorithm to find the optimal path has been presented in Fig. 1. In the first step, accuracy matrices and solution accuracy are selected. Then the initial and final condition of each link, θ_{i0}, θ_{if}, can be calculated by the inverse kinematic equation. The remaining generalized coordinate, $\dot{\theta}_{i0}, \dot{\theta}_{if}$ and q_{ij0}, q_{ijf}, can be considered equal to zero because of the rest-to-rest motion. Condition (I) in this algorithm is investigating the singularity conditions. If two selected points are not in the workspace or the Jacobian values at initial or final configuration is equal to zero, the algorithm jumps back to the second step and two new points should be selected. After selecting the penalty matrices values (W_1, W_2, and R), the two-point boundary value problem is solved and state X, Control U, and the other necessary terms such as power or energy are calculated. Condition (II) is as follows: if the desired objectives and purposes are satisfied with W_1, W_2, R, and violated (or became worse) with $W_1 \pm \delta W_1$, $W_2 \pm \delta W_2$, $R \pm \delta R$, the obtained path is the optimal and the running be stopped, otherwise, the algorithm jumps back to step four and the weighting factors are improved.

4.2. Optimal path for maximum payload

The proposed method to find the MADL of flexible manipulators provides the ability to determine the maximum payload for each considered performance measure. In other words, in addition to maximize the payload, other objectives can be achieved by defining the proper objective functions. The proposed algorithm shown in Fig. 2 can be used

https://doi.org/10.1017/S0263574708005183 Published online by Cambridge University Press

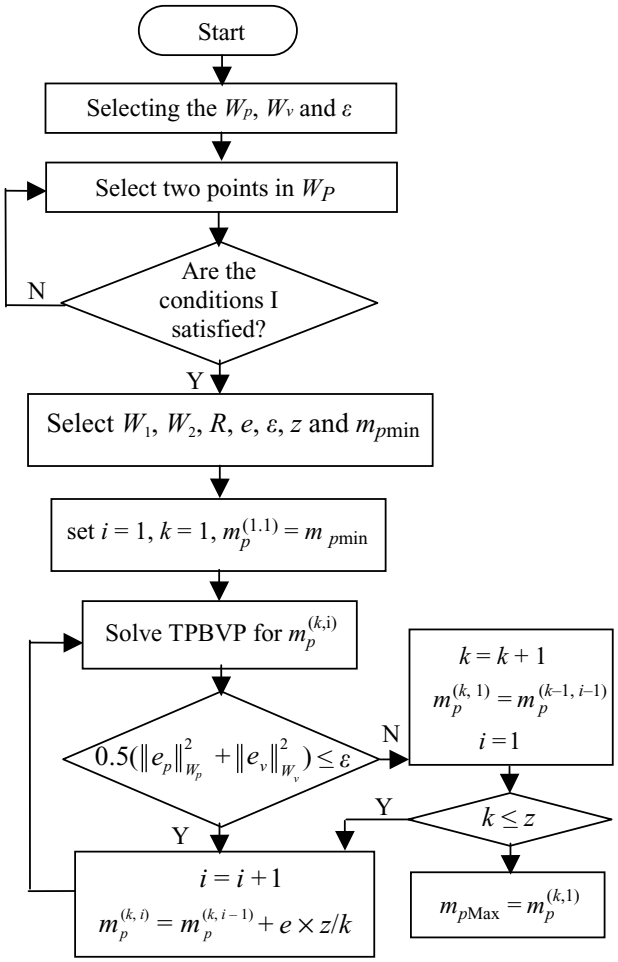

Fig. 2. Maximum payload algorithm.

to calculate the maximum payload and its corresponding optimal trajectory at point-to-point motion for a flexible-link manipulator. First to third steps of this algorithm are similar to the optimal path algorithm (Fig. 1). e is the accuracy at the payload calculation and z is the iteration number. The solution method is based on increasing the payload from its minimum value ($m_{p\min}$), until the maximum payload value can be found. For the sake of achieving the proper accuracy in payload calculation as well as getting the high approaching rate to final answer, the presented solution algorithm has two loops. One of them (i) increases the payload at each iteration and the other one (k) adjusts the jump interval. For the payload less than the maximum payload value ($m_p \le m_{p\max}$) attaining the desired accuracy ε in the TPBVP solution is possible, so the payload increases in each step in loop (i). But whenever the payload exceeds the maximum payload ($m_p > m_{p\max}$), the final error value obtained from Eq. (17), increases suddenly and loop (k) is acted. For $m_{p\max}$, the final error will be less than ε and the motors work on their maximum capacity. At this condition carrying the payload more than $m_{p\max}$ is required to applying torque more than their limits, but it is impossible because the torque constraints are satisfied from Eqs. (14) and (15) at each iteration in the TPBVP solution. Consequently, the error value becomes large significantly. By the use of this fact, a criterion for the maximum payload calculation is employed in the presented algorithm.

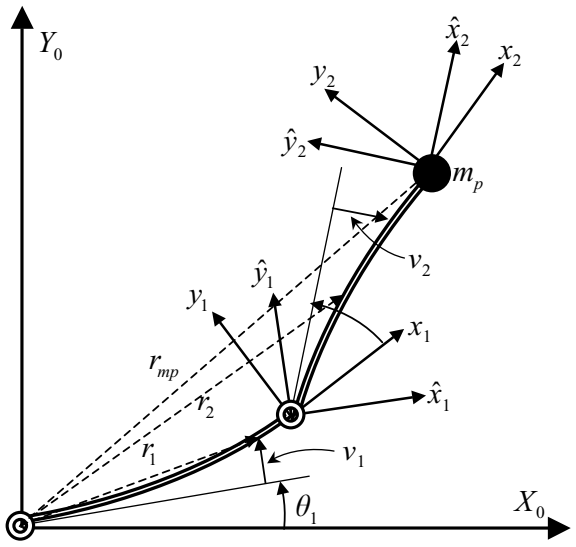

Fig. 3. Two-link manipulator with flexible links.

Table I. Simulation parameters.

Parameter	Value
Length of links (m)	$L_1 = L_2 = 0.5$
Mass (kg)	$m_1 = 3$, $m_2 = 3$
Moment of area (link; m^4)	$I_1 = I_2 = 2.5 \times 10^{-9}$
Module of elasticity (link; kg·m^2)	$E_1 = E_2 = \times 10^{-10}$
Max. no of load speed (Rad/s)	$\omega_{s1} = \omega_{s2} = 3.5$
Actuator stall torque (N·m)	$\tau_{s1} = \tau_{s2} = 8$

5. Simulation for a Two-Link Manipulator

5.1. Deriving the equations

A two-link manipulator with flexible link at horizontal plane with the associated coordinate system is shown in Fig. 3. A concentrated payload of mass m_p is connected to the second link. All the required parameters of the robot manipulator are given in Table I.[31] Using the generalized modeling scheme given in,[12,29] equations of motion of a manipulator with two flexible links are derived here.

Using the symbols defined in Fig. 3, the expressions for position vector r_1, r_2, and r_{mp} in the XY plane can be written as below:

$$r_1 = \begin{bmatrix} x_1 c_1 - v_1 s_1 \\ x_1 s_1 + v_1 c_1 \end{bmatrix},$$

$$r_2 = \begin{bmatrix} L_1 c_1 - v_{1L} s_1 + x_2 c_{12} - v_2 s_{12} \\ L_1 s_1 + v_{1L} c_1 + x_2 s_{12} + v_2 c_{12} \end{bmatrix},$$

$$r_{m_p} = \begin{bmatrix} L_1 c_1 - v_{1L} s_1 + L_2 c_{12} - v_{2L} s_{12} \\ L_1 s_1 + v_{1L} c_1 + L_2 s_{12} + v_{2L} c_{12} \end{bmatrix} \qquad (18)$$

where c_1, s_1, c_{12}, and s_{12} are shorthand expressions for $\cos(\theta_1)$, $\sin(\theta_1)$, $\cos(\theta_1 + \theta_2)$, and $\sin(\theta_1 + \theta_2)$, respectively. With a view to obtain a simplified model with reasonable

https://doi.org/10.1017/S0263574708005183 Published online by Cambridge University Press

accuracy, two modes per link are considered, so $v_i(x_i, t)$ can be given by

$$\begin{aligned} v_1 &= \phi_{11}(x_1)q_{11}(t) + \phi_{12}(x_1)q_{12}(t), \\ v_2 &= \phi_{21}(x_2)q_{21}(t) + \phi_{22}(x_2)q_{22}(t) \\ v_{1L} &= \phi_{11}(L_1)q_{11}(t) + \phi_{12}(L_1)q_{12}(t), \\ v_{2L} &= \phi_{21}(L_2)q_{21}(t) + \phi_{22}(L_2)q_{22}(t), \end{aligned} \tag{19}$$

where, while considering the simply support mode shape,[30] ϕ_{ij} can be computed as follows:

$$\phi_{ij}(x_i) = \sin(j\pi x_i/L_i), \quad i = 1, 2 \text{ and } j = 1, 2. \tag{20}$$

The kinetic energy of a point $r_i(x_i)$ on the links and payload can be written as

$$\begin{aligned} K_1 &= 0.5\rho_1 \int_0^{L_1} \dot{r}_1^T(x_1)\dot{r}_1(x_1)\,dx_1, \\ K_2 &= 0.5\rho_2 \int_0^{L_2} \dot{r}_2^T(x_2)\dot{r}_2(x_2)\,dx_2, \quad K_{mp} = 0.5m_p\dot{r}_{mp}^T\dot{r}_{mp} \end{aligned} \tag{21}$$

where ρ_i is the linear mass density for the ith link and $\dot{r}_i(x_i)$ is the velocity vector. The velocity vector can be computed by taking the time derivative of its position (18):

$$\begin{aligned} {}^0\dot{r}_1 &= \begin{bmatrix} -x_1\dot{\theta}_1 s_1 - v_1\dot{\theta}_1 c_1 - \dot{v}_1 s_1 \\ x_1\dot{\theta}_1 c_1 - v_1\dot{\theta}_1 s_1 + \dot{v}_1 c_1 \end{bmatrix} \\ {}^0\dot{r}_2 &= \begin{bmatrix} -L_1\dot{\theta}_1 s_1 - v_{1L}\dot{\theta}_1 c_1 - \dot{v}_{1L}s_1 - x_2(\dot{\theta}_1+\dot{\theta}_2)s_{12} \\ \quad - \dot{v}_2 s_{12} - v_2(\dot{\theta}_1+\dot{\theta}_2)c_{12} \\ L_1\dot{\theta}_1 c_1 - v_{1L}\dot{\theta}_1 s_1 + \dot{v}_{1L}c_1 + x_2(\dot{\theta}_1+\dot{\theta}_2)c_{12} \\ \quad + \dot{v}_2 c_{12} - v_2(\dot{\theta}_1+\dot{\theta}_2)s_{12} \end{bmatrix} \\ {}^0\dot{r}_{mp} &= \begin{bmatrix} -L_1\dot{\theta}_1 s_1 - v_{1L}\dot{\theta}_1 c_1 - \dot{v}_{1L}s_1 - L_2(\dot{\theta}_1+\dot{\theta}_2)s_{12} \\ \quad -\dot{v}_{2L} s_{12} - v_{2L}(\dot{\theta}_1+\dot{\theta}_2)c_{12} \\ L_1\dot{\theta}_1 c_1 - v_{1L}\dot{\theta}_1 s_1 + \dot{v}_{1L}c_1 + L_2(\dot{\theta}_1+\dot{\theta}_2)c_{12} \\ \quad + \dot{v}_{2L} c_{12} - v_{2L}(\dot{\theta}_1+\dot{\theta}_2)s_{12} \end{bmatrix} \end{aligned} \tag{22}$$

On the other hand, the potential energy due to the deformation of the first and second links can be written as

$$\begin{aligned} U_1 &= \frac{1}{2}E_1 I_1 \int_0^{L_1} \frac{\partial^2 v_1}{\partial^2 x_1^2} dx_1, \\ U_2 &= \frac{1}{2}E_2 I_2 \int_0^{L_1} \frac{\partial^2 v_2}{\partial^2 x_2^2} dx_2. \end{aligned} \tag{23}$$

where $E_i I_i$ is the flexural rigidity of the ith link and v_i is substituted from (19) and (20). Next, to obtain a closed-form dynamic model of the manipulator, the energy expressions (21) and (23) are used to formulate the Lagrangian $L = K_1 + K_2 + K_{mp} - (U_1 + U_2)$. Here the generalized coordinate vector consists of link positions (θ_1, θ_2) and modal displacements $(q_{11}, q_{12}, q_{21}, q_{22})$. The generalized force vector is $U = \{\tau_1, \tau_2, 0, 0, 0, 0\}^T$, where τ_1 and τ_2 are the torques applied by motor 1 and motor 2, respectively. Therefore, the following Euler–Lagrange's equations results, with $i = 1, 2$ and $j = 1, 2$:

$$\begin{aligned} &\frac{d}{dt}\left(\frac{\partial L}{\partial \dot{\theta}_i}\right) - \frac{\partial L}{\partial \theta_i} = \tau_i, \; \frac{d}{dt}\left(\frac{\partial L}{\partial \dot{q}_{1j}}\right) - \frac{\partial L}{\partial q_{1j}} = 0, \\ &\frac{d}{dt}\left(\frac{\partial L}{\partial \dot{q}_{2j}}\right) - \frac{\partial L}{\partial q_{2j}} = 0. \end{aligned} \tag{24}$$

The final dynamic equations of motion of the manipulator after algebraic simplifications can be put in a concise form as

$$\begin{bmatrix} J_{r11} & J_{r12} & J_{rf111} & J_{rf112} & J_{rf113} & J_{rf114} \\ & J_{r22} & J_{rf211} & J_{rf212} & J_{rf213} & J_{rf214} \\ & & J_{ff11} & J_{ff12} & J_{ff13} & J_{ff14} \\ & & & J_{ff22} & J_{ff23} & J_{ff24} \\ & \text{Sym.} & & & J_{ff33} & J_{ff34} \\ & & & & & J_{ff44} \end{bmatrix} \begin{bmatrix} \ddot{\theta}_1 \\ \ddot{\theta}_2 \\ \ddot{q}_{11} \\ \ddot{q}_{12} \\ \ddot{q}_{21} \\ \ddot{q}_{22} \end{bmatrix} + \begin{bmatrix} h_{r1} \\ h_{r2} \\ h_{f11} \\ h_{f12} \\ h_{f21} \\ h_{f22} \end{bmatrix} = \begin{bmatrix} \tau_1 \\ \tau_1 \\ 0 \\ 0 \\ 0 \\ 0 \end{bmatrix}, \tag{25}$$

where the values of inertia matrix are given in the appendix. Because of the very long terms of the Coriolis and centrifugal forces, they are neglected to bring in the paper text. Since the motion is in horizontal plane, the gravity effects (G_r, G_f) will be zero. By using Eqs. (3)–(5) and defining the state vectors as

$$\begin{aligned} X_1 &= Q^T = [\, x_1 \; x_3 \; x_5 \; x_7 \; x_9 \; x_{11} \,]^T \\ X_2 &= \dot{Q}^T = [\, x_2 \; x_4 \; x_6 \; x_8 \; x_{10} \; x_{12} \,]^T, \end{aligned} \tag{26}$$

the state-space form of Eq. (25) is written as

$$\dot{x}_{2i-1} = x_{2i}, \dot{x}_{2i} = F_2(i); i = 1, \ldots, 6, \tag{27}$$

where $F_2(i)$ can be obtained from Eq. (5). Now, in order to check the validity of the obtained model, the simulation conditions done in ref. [31] are considered. Model verification is supported by comparing the response of the flexible arm model with that of the rigid one. Clearly, as the flexural rigidity, EI, of the links increase, joint angle response of the flexible model should converge to that of the rigid model. In this simulation, the harmonic motion of the two-link manipulator hanging freely under gravity is obtained at the initial conditions corresponding to $\theta_1(0) = -1.5$ rad and $\theta_2(0) = -0.5$ rad. The joint angles of the rigid manipulator and flexible one are shown in Fig. 4. As it can be seen the response of the flexible manipulator with $EI = 100$ is very close to the rigid manipulator response. Also the results are in good agreement with the similar case done in ref. [31].

After verifying the dynamic model, a point-to-point motion is considered. The initial position of the end-effector in XY plane at $t = 0$ is $p_0 = (0.5, 0)$, the final position at $t = 1$ s

https://doi.org/10.1017/S0263574708005183 Published online by Cambridge University Press

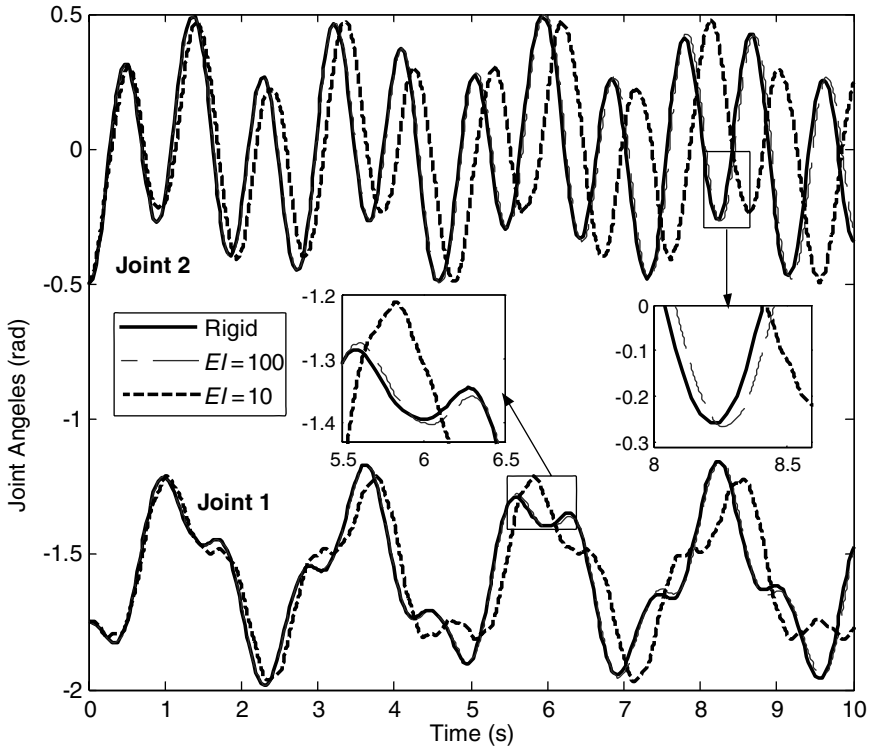

Fig. 4. The joint angle responses of two-link flexible model, pinned-pinned modes shapes.

is $p_f = (0.5, 0.5)$ and the initial and final velocity are zero, therefore using inverse kinematic equations, the boundary condition can be expressed as follows:

$$\begin{aligned} &x_{10} = 60^\circ, x_{30} = -60^\circ; \quad x_{1f} = 90^\circ, \quad x_{3f} = -90^\circ \\ &x_{2i0} = x_{2if} = 0, \quad i = 1, \ldots, 6; \\ &x_{(2i-1)0} = x_{(2i-1)f} = 0, \quad i = 3, \ldots, 6. \end{aligned} \tag{28}$$

In order to derive the equations associated with optimality conditions, penalty matrices are selected as

$$\begin{aligned} W_1 &= \text{diag}(w_1, w_3, w_5, w_7, w_9, w_{11}) \\ W_2 &= \text{diag}(w_2, w_4, w_6, w_8, w_{10}, w_{12}), \\ R &= \text{diag}(r_1, r_2). \end{aligned} \tag{29}$$

Then, the objective function is obtained by substituting Eq. (29) into Eq. (7) as

$$L = \frac{1}{2}\left(r_1\tau_1^2 + r_2\tau_2^2 + \sum_{i=1}^{12} w_i x_i^2\right). \tag{30}$$

By considering the costate vector as $\psi^T = [\varphi_i]^T, i = 1, \ldots, 12$, and substituting for L from (30) and for $\dot{x}_i, i = 1, \ldots, 12$ from (27) into Eq. (8), the Hamiltonian function becomes

$$H = \frac{1}{2}\left(r_1\tau_1^2 + r_2\tau_2^2 + \sum_{i=1}^{12} w_i x_i^2\right) + \sum_{i=1}^{12} \varphi_i \dot{x}_i. \tag{31}$$

Consequently, the costate equations can be obtained using Eq. (9) by differentiating the Hamiltonian function with respect to the states as follows:

$$\dot{\varphi}_i = -\frac{\partial H}{\partial x_i}, \quad i = 1, \ldots, 12. \tag{32}$$

The control equations can be computed using Eq. (14) by differentiating the Hamiltonian function with respect to the controls (τ_1, τ_2). After that, from Eq. (15) the extremal bound of control for each motor becomes

$$\begin{aligned} U_1^+ &= k_{11} - k_{12}x_2, \quad U_1^- = -k_{11} - k_{12}x_2, \\ U_2^+ &= k_{21} - k_{22}x_4, \quad U_2^- = -k_{21} - k_{22}x_4. \end{aligned} \tag{33}$$

By substituting the obtained control equations in (27) and (32), these equations forms 24 nonlinear ordinary differential equations which with 24 boundary conditions given in (26), constructs a two-point boundary value problem. This problem can be solved using the BVP4C command in MATLAB®.

5.2. Minimum effort-speed trajectory

The path with minimum effort is a path in which the minimum torque is exerted by each motor. In this case, the magnitudes of the motors velocity are not important, while they may exceed the allowable maximum speeds. In order to solve this problem, the performance measure can be defined as follows:

$$J_0(U) = 0.5 \int_{t_0}^{t_f} \left(U^T R U + X_2^T W_2 X_2\right) dt \tag{34}$$

https://doi.org/10.1017/S0263574708005183 Published online by Cambridge University Press

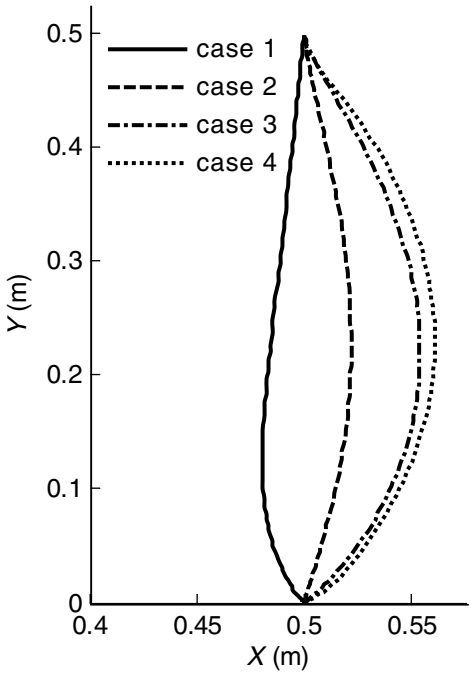

Fig. 5. End effector trajectory in *XY* plane.

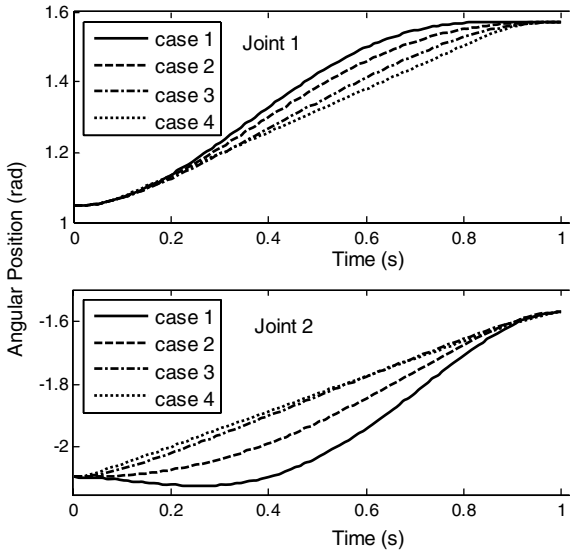

Fig. 6. Angular positions of joint 1 and 2.

in which the velocity of motors can be reduced via increasing the penalty matrix corresponding to the angular velocity of motors (W_2). In order to show this aspect, the following problem is planned. We find the optimal path between p_0 (0.5, 0) and p_f (0.5, 0.5) in such a way that the smallest amount control value can be applied and the angular velocity of motors be bounded in ± 0.8 rad/s. The payload is considered to be 1 kg.

In order to solve this problem, the accuracy matrices are considered to be $W_p = W_v = \text{diag}(1)$ and the solution accuracy ε is 0.001. By considering the penalty matrices as $W_1 = W_2 = 0$, $R = \text{diag}(1/8)$, the optimal path with minimum effort can be obtained, but the angular velocities are greater than 0.8 rad/s. Therefore for decreasing the velocities, W_2 must be increased. A range of values of $W_2 = (w_2, w_2, 0, 0, 0, 0)$ used in simulation are given in Table II. W_1 and R remain without changes.

Table II. The values of w_2 used in the simulation.

case	1	2	3	4
w_2	0	1	10	1400

The end-effector trajectories in *XY* plane for these cases are shown in Fig. 5. Figure 6 shows the angular position of joints with respect to time. This graph shows that by increasing the W_2, the angular position becomes approximately a straight line. Figure 7 shows the angular velocities of the first and second joints. It can be found that increasing the W_2 leads to reduce the exterimum values of angular velocities from 1.2 rad/s to 0.6 rad/s. By increasing the W_2, the angular

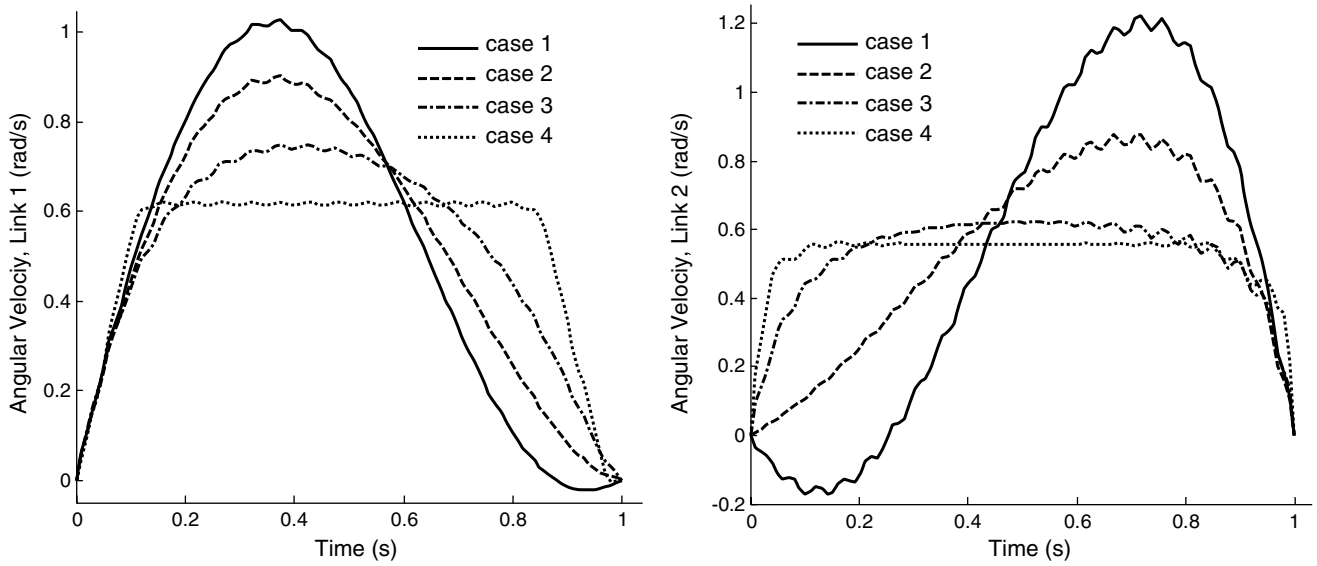

Fig. 7. Angular velocities of joint 1 and 2.

https://doi.org/10.1017/S0263574708005183 Published online by Cambridge University Press

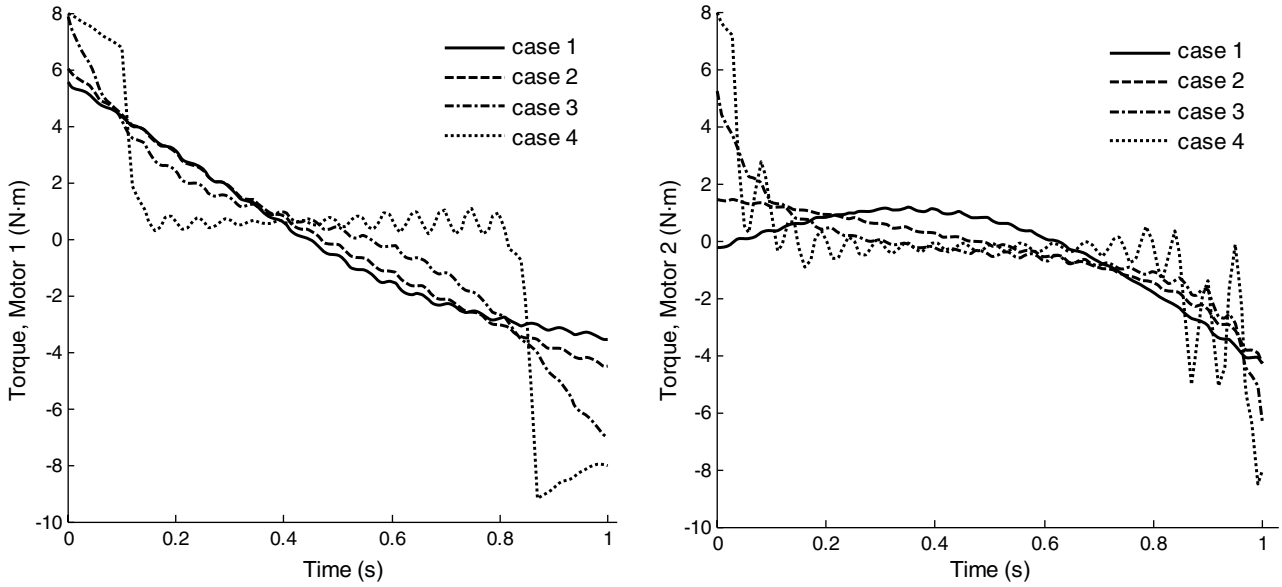

Fig. 8. Torque curves of motor 1 and 2.

velocities reduce greatly for the first to third cases whereas at the fourth case a little reduction has been occurred in spite of the great increase in W_2. At this condition, decrease in the angular velocities less than 0.6 rad/s is not possible. Because by considering the W_2 larger than 1400, the TPBVP solution cannot converge to desired accuracy ε. Consequently, the desired condition for angular velocities, $-0.8 \leq \dot{\theta}_1, \dot{\theta}_2 \leq 0.8$, is accomplished for the third case ($w_2 = 10$). The computed torque is plotted in Fig. 8. As it can be seen, increasing the W_2 causes to raise the torques, so that for the last case the torque curves reach to their bounds at the beginning and end of the path. This result is predictable, because increasing the W_2 decreases the proportion of weighting matrix R and the result of this is increasing the control values.

Therefore, the first path is the optimal path with the least control values, whereas its angular velocity is of the largest magnitude. Finally, for the considered problem, the optimal path is the third one in which its velocity magnitudes are bounded in ± 0.8 rad/s interval and its torque values are the lowest. On the basis of the objective contrast principle, there is not a solution that satisfies all the desired objectives simultaneously. For example the optimal path with minimum effort has the maximum velocity and the optimal path with minimum velocity has the maximum effort. Consequently, in this method, designer compromises between the different objectives by considering the proper penalty matrices.

5.3. Maximum payload trajectory

In this section finding the maximum payload value carried between the initial and final point, p_0 (0.5, 0) and p_f (0.5, 0.5) are presented. Using the obtained equations at Section 4 and on the basis of the presented algorithm in Fig. 3, m_p increases from $m_{p\min}$, until $m_{p\max}$ is obtained. Desired accuracy in the TPBVP solution and payload calculation is considered as $\varepsilon = 0.001$ and $e = 0.05$. The penalty matrices are considered to be $W_p = W_v = \text{diag}(1)$, $W_1 = W_2 = \text{diag}(0)$, and $R = \text{diag}(1/8)$. The maximum payload for these values of penalty matrices is found to be 5.85 kg. The torque curves of the first and second joints for a range of m_p given in Table III are shown in Fig. 9.

Table III. The values of m_p used in the simulation.

4	3	2	1	i
5.85	5.5	4	1	m_p (kg)

Table IV. The values of w_2 used in the simulation.

4	3	2	1	i
1000	700	200	0	w_2
4.6	5.1	5.5	5.85	$m_{p\max}$ (kg)

Figure 9 shows how the maximum payload trajectory is obtained on the basis of the algorithm given in Fig. 2. As it can be seen, increasing the payload increases the required torque until the torque curves lay on their own limits completely. For $m_p = 5.85$ kg, the most possible values of the torques are applied and increasing the payload more than this value requires to applying torque beyond the limits. Because the torque constraints are satisfied in each step of the TPBVP solution, increasing the payload more than m_{pmax} leading to violate the boundary conditions at t_f, so the solution cannot converge to the desired accuracy ε.

$m_{p\max} = 5.85$ kg is the maximum payload for the considering penalty matrices while choosing the other penalty matrices, results in other optimal trajectories. To illustrate this aspect, some simulations are done for different values of $W_2 = (w_2,\ w_2,\ 0,\ 0,\ 0,\ 0)$ given in Table IV. In this Table, w_2 and the calculated maximum payload for each case is indicated. The other penalty matrices remain without changes: $W_1 = [0]$ and $R = \text{diag}(1/8)$.

https://doi.org/10.1017/S0263574708005183 Published online by Cambridge University Press

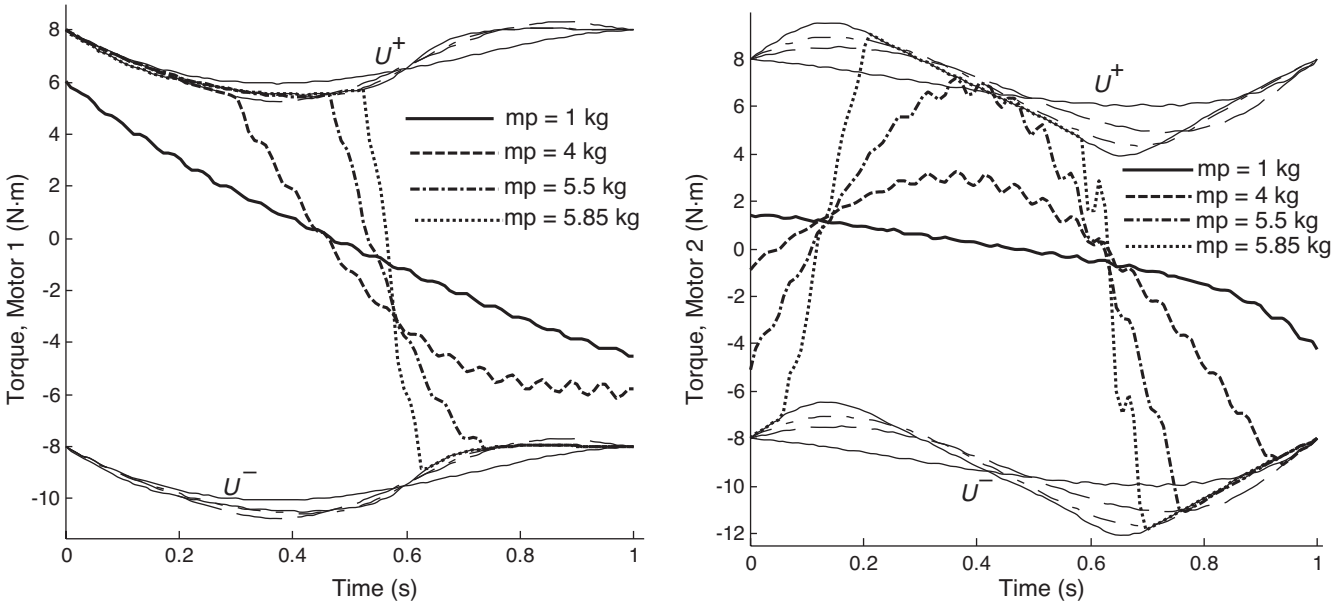

Fig. 9. Torque curves of motor 1 and 2.

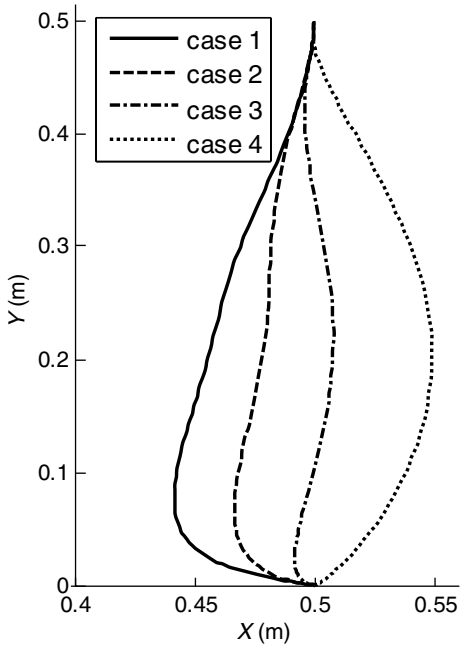

Fig. 10. Maximum payload trajectories.

Figure 10 shows the different maximum payload trajectories in XY plane. The corresponding joint angular velocities are illustrated in Fig. 11. As it is expected, by increasing the W_2 the velocity values decrease and various optimal paths have been attained. The torque curves and their bounds are shown in Fig. 12. This simulation test shows that by selecting the different objective functions, different maximum payload-optimal paths are obtained. All of the curves in Fig. 10 are optimal paths with maximum payload, which depends on the limitations in workspace or other wanted requirements, each of them may be selected.

In order to investigate the link flexibility on the maximum payload value, and check the performance of the method for different amount of elasticity, simulation is performed for the various stiffness properties. The same physical properties shown in Table I and the same initial and final position are considered for the simulation conditions. Penalty matrices are considered to be: $W_1 = W_2 = [0]$ and $R = \text{diag}(1/8)$. The values of stiffness EI, and the corresponding maximum payloads are given in Table V.

Table V. Maximum payload for different stiffness.

i	1	2	3
EI (N·m^2)	rigid	50	5
m_{pmax} (kg)	5.85	5.8	5.75

It is found that the maximum payload for flexible cases are approximately close to the rigid case and decreasing the rigidity leads to a fewer maximum payload. The maximum payload paths for these cases are shown in Fig. 13 and the torque curves are given in Fig. 14. It can be seen that the oscillation of torque curves becomes more by decreasing the stiffness value.

5.4. Minimum effort trajectory

In order to verify the method, in this section simulation is performed for a flexible manipulator studied in ref. [17] and the obtained results from the proposed method are compared with it. The parameters of this manipulator are given in Table VI. A schematic view of this robot is also shown in Fig. 15. Problem is to find the optimal path with minimum effort, so penalty matrices can be considered to be $R = \text{diag}(1)$, $W_1 = [0]$ and $W_2 = [0]$. One simply support mode shape for each link is considered. The system is initially at rest, thus the initial conditions are $\theta_1(0) = \dot{\theta}_1(0) = \dot{\theta}_2(0) = 0, \theta_2(0) = 180^\circ$. The final time is set to $t_f = 2.0$ s and the final conditions are $\theta_2(t_f) = \dot{\theta}_1(t_f) = \dot{\theta}_2(t_f) = 0, \theta_1(t_f) = 180^\circ$. So the 16 boundary conditions can be considered as follows:

$$\begin{aligned} &x_{10} = 0, x_{30} = 180^\circ; \quad x_{1f} = 180^\circ, x_{3f} = 0 \\ &x_{i0} = x_{if} = 0, i = 2, 4; \quad x_{i0} = x_{if} = 0, i = 5, \ldots, 8 \end{aligned} \tag{35}$$

https://doi.org/10.1017/S0263574708005183 Published online by Cambridge University Press

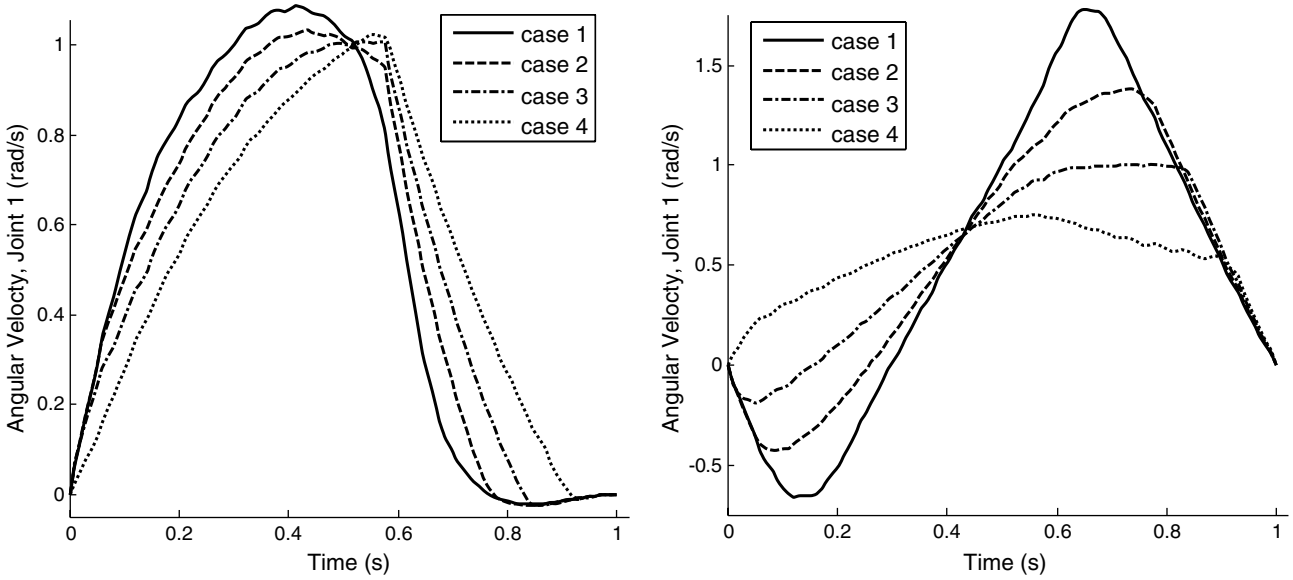

Fig. 11. Angular velocities of joint 1 and 2.

Table VI. Physical parameters of flexible manipulator.

Description	Symbol	Value
Thickness, Links 1 and 2 (mm)	t_1, t_2	5.537, 1.574
Length, Links 1 and 2 (m)	L_1, L_2	0.5969, 0.4842
Width, Links 1 and 2 (m)	w_1, w_2	0.1524, 0.0762
Moment of inertia (kg·m^2)	J_1, J_2, J_3	1, 1, 1
Mass at 2nd, 3rd nodes (kg)	m_2, m_3	5.415, 0.83
Viscous friction, Joint 1 and 2 (kg·m^2/s)	c_1, c_2	0.05, 0.05
Density of links (kg/m)	ρ	2700
Modulus of elasticity (N/m^2)	E	6.9×10^{-10}

The upper and lower bounds of each motor are $U_{\max,\min 1} = \pm 13.5\,\mathrm{N \cdot m}$ and $U_{\max,\min 2} = \pm 4.0\,\mathrm{N \cdot m}$. The obtained results of this simulation are shown in Fig. 16. The angular positions of links, corresponding velocities and the minimum effort torque profiles are shown in this figure. Note that for torque profiles, each actuator saturates at the maximum and minimum bounds at the beginning and the end of the maneuver, respectively. The obtained results from the proposed method given in Fig. 16 show a reasonable agreement with those reported in ref. [17]. With a rough comparison, the features of velocity and torque curves in both the different methods are similar to each others. Also, the amplitude and frequency of oscillations in velocity and torque curves in Fig. 16 are equal to the ones given in ref. [17]. The other parameters such as the maximum velocities and the rate of the torque curves are equal in both methods.

5.5. Minimum vibration trajectory

An important path planning problem for flexible manipulators studied by many researchers is to obtain

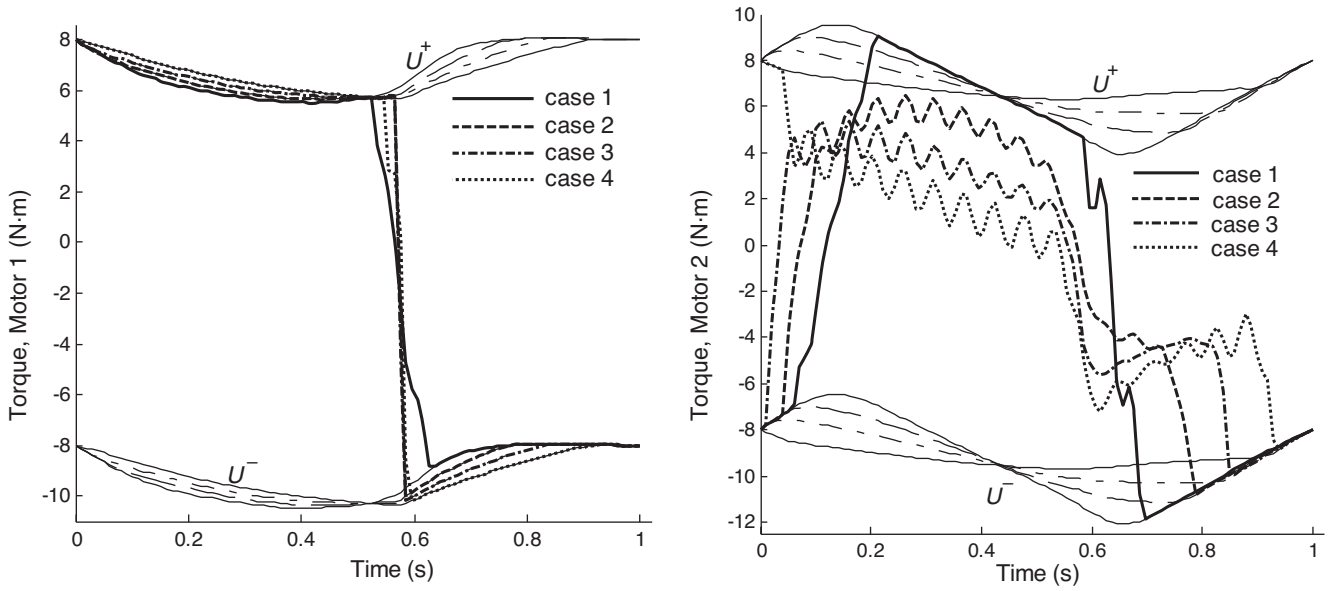

Fig. 12. Torque curves of motor 1 and 2.

https://doi.org/10.1017/S0263574708005183 Published online by Cambridge University Press

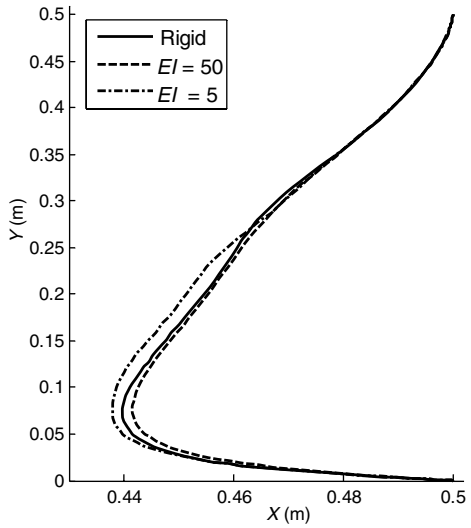

Fig. 13. Maximum. payload trajectories for different stiffness.

the minimum vibration trajectory.[14–16] In this section, this problem is considered and the ability of the proposed method to solve it is shown. Simulations are performed for two cases. In the first case weighting factors are selected as $R = \text{diag}(1)$, $W_1 = [0]$, and $W_2 = [0]$, which is the minimum effort trajectory, and in the second case weighting factors are considered to be: $R = \text{diag}(1)$, $W_1 = [0]$, and $W_2 = \text{diag}(0, 0, 500, 500)$. By increasing the weighting factors corresponding to the derivative of mode shapes ($\dot{q}_{11}, \dot{q}_{21}$), the vibrational motions will be suppressed. The bounds on the motors capacity are not considered. The results of these simulations are illustrated in Figs. 17–20. The velocity and torque curves are given in Fig. 17. As it can be seen, for the minimum vibration trajectory, the oscillation amplitudes in velocity curves has been reduced considerably, but the magnitude of motor torques has been increased. It means that for achieving a smoother path, more effort must be applied. The mode shapes and the derivations are given in Fig. 18. It is observed that the mode shape amplitudes for the minimum vibration

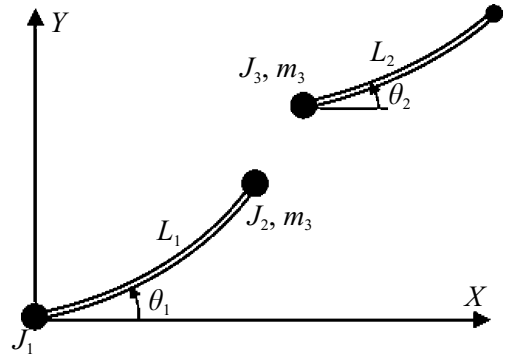

Fig. 15. Schematic view of two-link manipulator.

trajectory are much less than the minimum effort trajectory. It is difficult to identify the frequency components by looking at the mode shape curves. Converting to the frequency domain, the discrete Fourier transform of the mode shapes is found by taking the 500-point fast Fourier transform. The power spectrum, the power measurement of the mode shapes at various frequencies, has been demonstrated in Fig. 19. Finally the end effector path in *XY* plane is shown in Fig. 20. It is clearly observed that the minimum vibration path is smoother than the minimum effort path.

Conclusion

In this paper, formulation of the trajectory optimization and finding the maximum payload trajectory for multiple flexible links manipulator in point-to-point motion, based on the indirect solution of optimal control problem is presented. After deriving the dynamic equation using the combined Euler–Lagrange formulation and assumed modes method, optimality conditions are applied using the PMP. The obtained equations lead to a standard form of a two-point boundary value problem for which several commands in different software such as MATLAB are available to solve it. An efficient algorithm based on the solution of two-point boundary value problem is proposed to optimize the path in

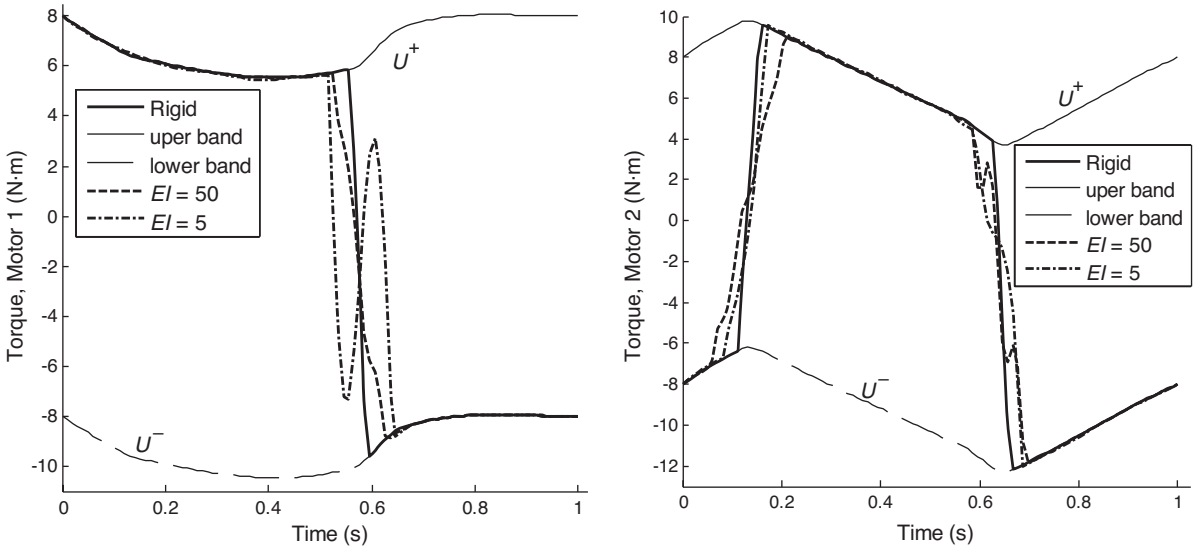

Fig. 14. Torques of motor 1 and 2 for different stiffness.

https://doi.org/10.1017/S0263574708005183 Published online by Cambridge University Press

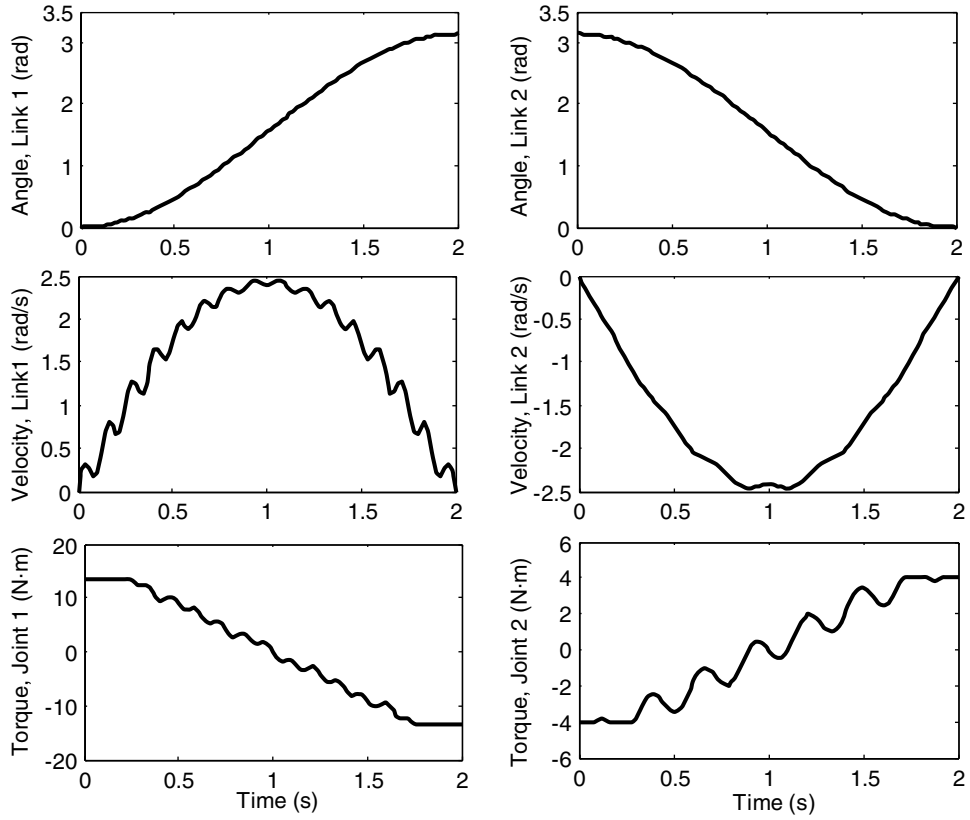

Fig. 16. Minimum effort results.

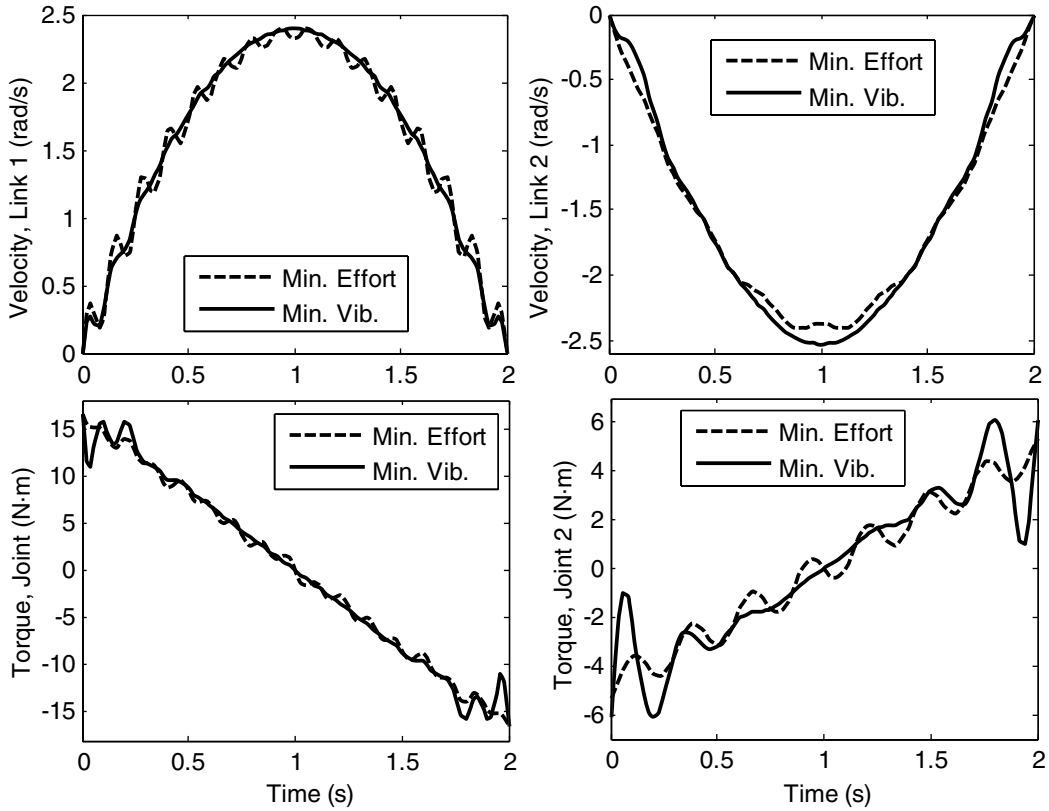

Fig. 17. Minimum vibration results.

https://doi.org/10.1017/S0263574708005183 Published online by Cambridge University Press

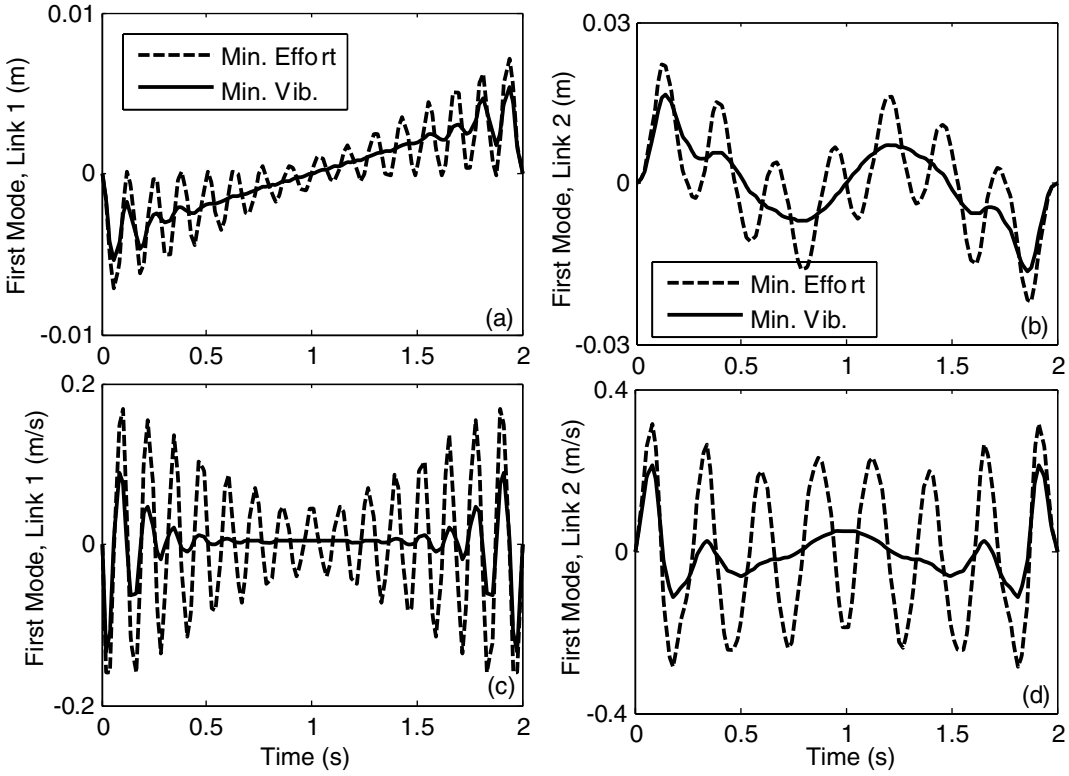

Fig. 18. Mode shapes of first and second link.

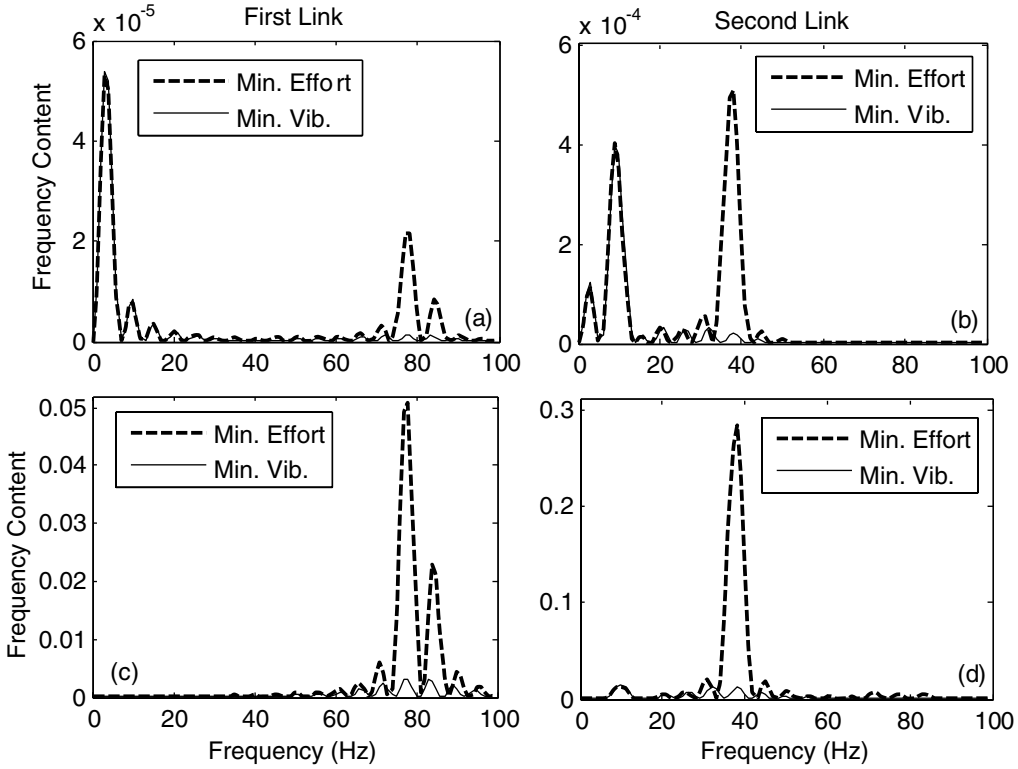

Fig. 19. The frequency content of mode shapes: (a) first mode of link 1; (b) first mode of link 2; (c) first mode derivation of link 1; (d) first mode derivation of link 2.

order to achieve the predefined objective. Another algorithm is then developed to calculate the maximum payload trajectory between two given points in the workspace. The efficiency of the proposed method is investigated through computer simulations by considering a simplified case study of a two-link flexible manipulator. It is shown that how this method is able to solve different path planning problem especially the maximum payload trajectory. In

https://doi.org/10.1017/S0263574708005183 Published online by Cambridge University Press

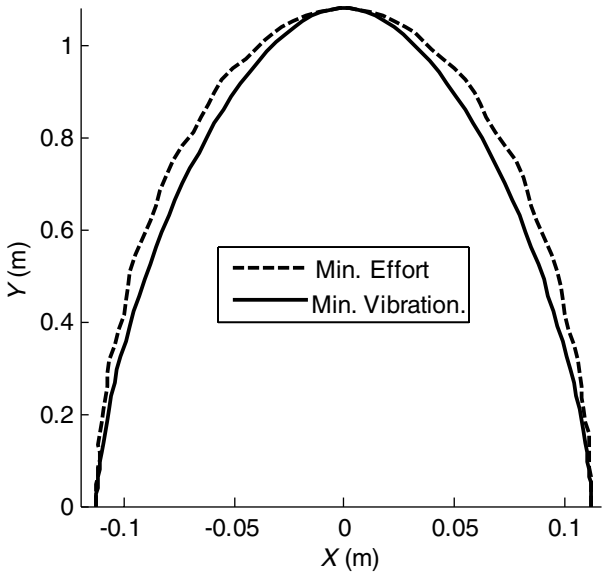

Fig. 20. End effector path in *XY* plane.

these simulations, minimum effort, minimum effort-speed, maximum payload, and minimum vibration problems are studied. Minimum effort case is performed in order to verify the method, and the obtained results are compared with those reported in ref. [17]. In minimum effort-speed case, an objective function consists of torque and speed is considered to obtain a minimum effort optimal path in the presence of limitations on joint angular velocities. In other simulation, the maximum payload trajectory using the proposed algorithm is obtained. It is observed that different maximum payload path can be attained which depends on the wanted requirements, each of them may be selected. Also, in order to investigate the link flexibility on the maximum payload trajectory, simulations are performed for a rigid link manipulator and two different values of stiffness. Finally, the minimum vibration problem is solved and it is shown that applying the proper input torque can decrease the end effector vibration significantly. The obtained results illustrate the power and efficiency of the method to overcome the high nonlinearity nature of the optimization problem which with other methods may be very difficult or impossible. The optimal trajectory and corresponding input control obtained using this method can be used as a reference signal and feedforward command in control structure of flexible manipulators.

References

1. J. Angeles, *Fundamentals of Robotic Mechanical Systems. Theory, Methods, and Algorithms* (Springer-Verlag, New York, 1997).
2. T. Chettibi, H. E. Lehtihet, M. Haddad and S. Hanchi, "Minimum cost trajectory planning for industrial robots," *Euro. J. Mech. A/Solids* **23**, 703–715 (2004).
3. L. T. Wang and B. Ravani, " Dynamic load carrying capacity of mechanical manipulators-Part 1," *J. Dyn Syst. Meas. Control* **110**, 46–52 (1988).
4. L. T. Wang and B. Ravani, "Dynamic load carrying capacity of mechanical manipulators-Part 2," *J. Dyn. Syst. Meas. Control* **110**, 53–61 (1988).
5. M. H. Korayem and H. Ghariblu, "Maximum allowable load of mobile manipulator for two given end points of end-effector," *Int. J. AMT* **24**(9–10), 743–751 (2004).
6. C.-Y. E. Wang, W. K. Timoszyk and J. E. Bobrow, "Payload maximization for open chained manipulator: Finding motions for a Puma 762 robot," *IEEE Trans. Rob. Autom.* **17**(2), (2001).
7. M. H. Korayem and A. Basu, "Formulation and numerical solution of elastic robot dynamic motion with maximum load carrying capacities," *Robotica* **12**, 253–261 (1994).
8. M. H. Korayem and A. Nikoobin, "Maximum payload for flexible joint manipulators in point-to-point task using optimal control approach," *Int. J. Adv. Manuf. Tech.* **38**(9–10), 1045–1060 (2008).
9. M. H. Korayem and H. Gariblu, "Analysis of wheeled mobile flexible manipulator dynamic motions with maximum load carrying capacities," *Rob. Auton. Syst.* **48**(2–3), 63–76 (2004).
10. H. Gariblu and M. H. Korayem, "Trajectory optimization of flexible mobile manipulators," *Robotica* **24**(3), 333–335 (2006).
11. S. Yue, S. K. Tso and W. L Xu, "Maximum dynamic payload trajectory for flexible robot manipulators with kinematic redundancy," *Mech. Mach. Theory* **36**, 785–800 (2001).
12. W. J. Book, "Recursive Lagrangian dynamics of flexible manipulator arms," *Int. J. Rob. Res.* **3**(3), 87–101 (1984).
13. D. G. Hull, "Conversion of optimal control problems into parameter optimization problems," *J. Guid. Control Dyn.* **20**(1), (1997).
14. P. K. Sarkar, M. Yamamoto and A. Mohri, "On the trajectory planning of a planar elastic manipulator under gravity," *IEEE Trans. Rob. Autom.* **15**(2), (1999).
15. H. Kojima and T. Kibe, "Optimal Trajectory Planning of a Two Link Flexible Robot Arm Based on Genetic Algorithm for Residual Vibration Reduction," *IEEE/RSJ International Conference on Intelligent Robots and Systems*, Maui, HI, vol. 4 (2001), pp. 2276–2281.
16. K. J. Park, "Flexible robot manipulator path design to reduce the endpoint residual vibration under torque constraints," *J. Sound Vib.* **275**, 1051–1068 (2004).
17. D. G. Wilson, R. D. Robinett and G. R. Eisler, "Discrete Dynamic Programming for Optimized Path Planning of Flexible Robots," *IEEE/RSJ International Conference on Intelligent Robots and Systems*, Sendai, Japan, vol. 3 (2004), pp. 2918–2923.
18. R. Luus, " Iterative dynamic programming," *Automatica* 39(7), 1315–1316 (2003).
19. J. Arora, *Introduction to Optimum Design*, 2nd Ed. (Elsevier, Academic Press, Sandiego, 2004).
20. D. E. Kirk, *Optimal Control Theory, an Introduction* (Prentice-Hall Inc., New Jersey, 1970).
21. Z. Shiller and S. Dubowsky, "Robot path planning with obstacles, actuators, gripper and payload constraints," *Int. J. Rob. Res.* **8**(6), 3–18 (1986).
22. R. Fotouhi and W. Szyszkowski, "An algorithm for time-optimal control problems," *J. Dyn. Syst. Meas. Control Trans. ASME* **120**(3), 414–418 (1998).
23. O. P. Agrawal and Y. Xu, "On the global optimum path planning for redundant space manipulators," *IEEE Trans. Syst. Man Cybernet.* **24**(9), (1994).
24. S. Furuno, M. Yamamoto and A. Mohri, "Trajectory Planning of Mobile Manipulator With Stability Considerations," *Proceedings of the 2003 IEEE International Conference on Robotics and Automation*, Taipei, Taiwan, vol. 3(14–19) (2003), pp. 3403–3408.
25. G. Bessonnet and S. Chessé, "Optimal dynamics of actuated kinematic chains, Part 2: Problem statements and computational aspects," *Euro. J. Mech. A/Solids* **24**, 472–490 (2005).
26. E. Bertolazzi, F. Biral and M. Da Lio, "Symbolic–numeric indirect method for solving optimal control problems for large multibody systems," *Multibody Syst. Dyn.* **13**(2), (2005).
27. M. R. Sentinella and L. Casalino, "Genetic Algorithm and Indirect Method Coupling for Low-Thrust Trajectory Optimization," *42nd AIAA/ASME/SAE/ASEE Joint Propulsion Conference and Exhibit*, California (2006).

https://doi.org/10.1017/S0263574708005183 Published online by Cambridge University Press

28. L. F. Shampine, M. W. Reichelt and J. Kierzenka, "Solving boundary value problems for ordinary differential equations in MATLAB with bvp4c," available at http://www.mathworks.com/bvp_tutorial
29. C.-J. Li and T. S. Sankar, "A systematic method of dynamics for flexible robot manipulators," *J. Rob. Syst.* **9**(7), 861–891 (1992).
30. A. Green and J. Z. Sasiadek, "Robot Manipulator Control for Rigid and Assumed Mode Flexible Dynamics Models," *AIAA Guidance, Navigation, and Control Conference and Exhibit*, Austin, TX, Paper no AIAA 2003–5435 (2003).
31. S. Cetinkunt and W. J. Book, "Symbolic modeling and dynamic simulation of robot manipulators with compliant links and joints," *Rob. Comput. Integr. Manuf.* **5**(4), 301–310 (1989).

Appendix

The inertia matrix components in Eq. (25) are obtained as follows:

$$
\begin{aligned}
J_{r11} &= (\rho/6)\big(3L_1q_{12}^2 + 3L_2q_{22}^2 + 3L_1q_{11}^2 + 2L_1^3 + 3L_2q_{21}^2 \\
&\quad - (24L_2L_1q_{21}\sin(\theta_2))/\pi + 6L_2L_1^2 + 2L_2^3 + 6L_2^2L_1 \\
&\quad \times \cos(\theta_2)\big) + \big(m_pL_1^2 + 2m_pL_1L_2\cos(\theta_2)\big) + m_pL_2^2 \\
J_{r12} &= L_2\big(\rho\big(-12L_1q_{21}\sin(\theta_2)/\pi + 3q_{22}^2 + 3L_2L_1\cos(\theta_2) \\
&\quad + 2L_2^2 + 3q_{21}^2\big)/6 + m_pL_1\cos(\theta_2) + mpL_2\big) \\
J_{r22} &= \rho L_2\big(3q_{21}^2 + 3q_{22}^2 + 2L_2^2\big)/6 + m_pL_2^2 \\
J_{ff11} &= J_{ff33} = \rho L_1/2; \quad J_{ff22} = J_{ff44} = \rho L_2/2 \\
J_{rf111} &= \rho L_1^2/\pi; \quad J_{rf112} = \big(L_2^2 + 2L_2L_1\cos(\theta_2)\big)/(\rho/\pi) \\
J_{rf113} &= -\rho L_1^2/(2\pi); \quad J_{rf114} = J_{rf214} = -\rho L_2^2/(2\pi) \\
J_{rf211} &= J_{rf213} = J_{ff12} = J_{ff13} = J_{ff14} \\
&= J_{ff23} = J_{ff24} = J_{ff34} = 0; \\
J_{rf212} &= \rho L_2^2/\pi
\end{aligned}
$$

https://doi.org/10.1017/S0263574708005183 Published online by Cambridge University Press